Nonlinear Frequency Domain Methods Applied to the Euler and Navier-Stokes Equations

Matthew McMullen

Advisor: Antony Jameson

Co-advisor: Juan Alonso

Sponsor: Accelerated Strategic Computing Initiative (ASCI) Project - DOE

Department of Aeronautics and Astronautics

Stanford University

Introduction

- The goal of ASCI is to perform numerical simulations of the unsteady flows inside an aircraft gas turbine engine.
- Estimates of the amount of work required for a single component simulation are provided below (Source: Davis 2001).

Component	Blade Rows	Grid Points (million)	Wheel Fraction	CPU Hours (million)	Execution Duration (days)
Turbine	9	94	$\frac{1}{6}$	3.0	510[1]
Compressor	23		$\frac{1}{6}$	7.7	1300[1]

[1] Based on 750 processors (1998 IBM SP2) working 8 hours per day.

- The goal of this research is to develop faster algorithms for unsteady flow calculations. We will focus on improving the efficiency of temporal discretizations and will not address spatial operators.

Time Accurate vs Periodic

- The previous time estimates are based on a time accurate solver (TFLO). This research will propose a periodic solver capable of solving nonlinear equations in the frequency domain.

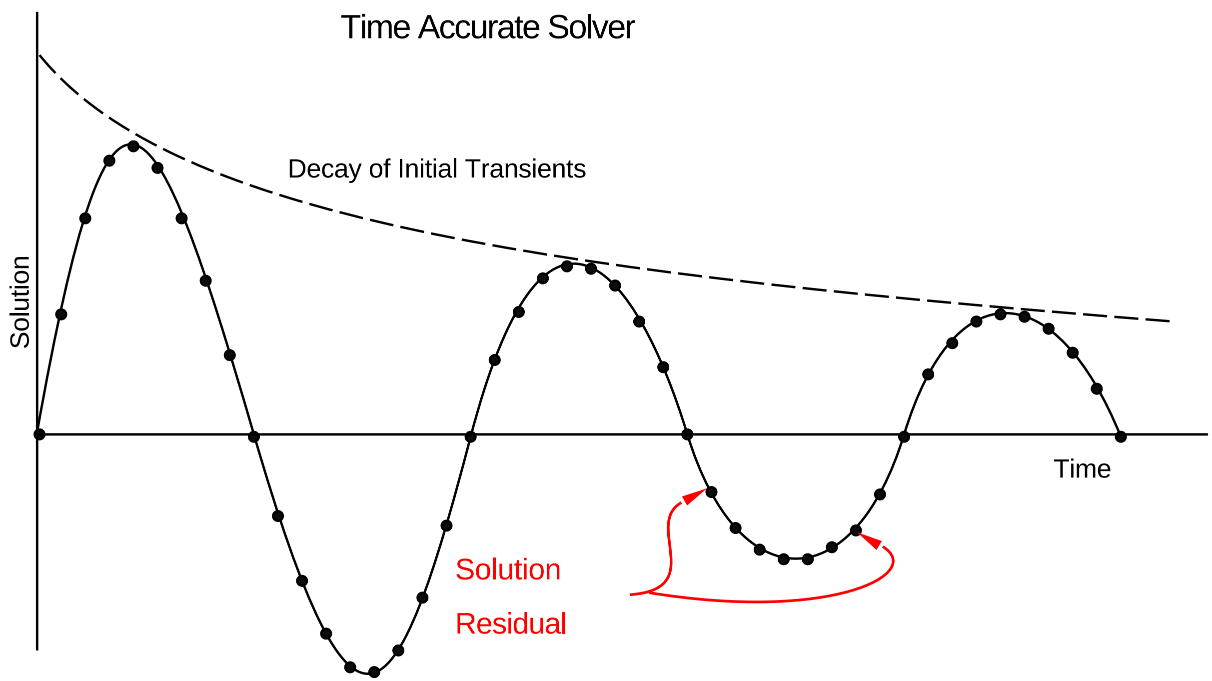

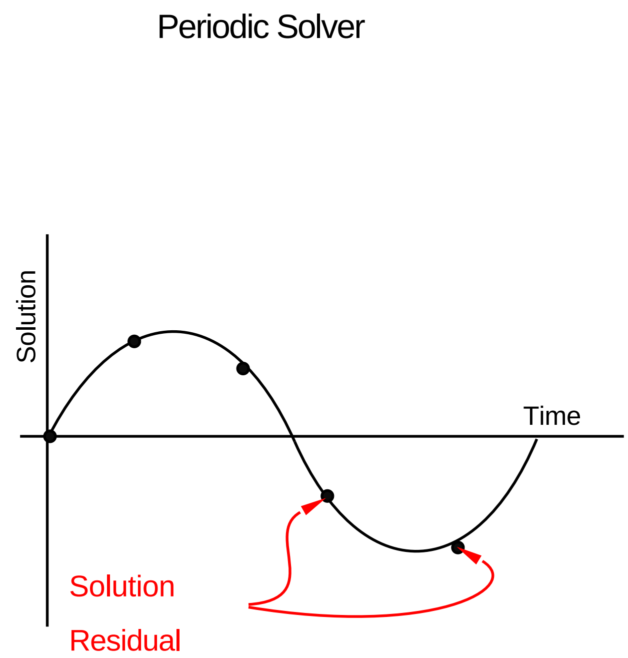

Outline

- Non-Linear Frequency Domain (NLFD) Solver
  Governing Equations
  Discretization
  Gradient Based Variable Time Period (GBVTP) Method
  Convergence Acceleration Issues
- Laminar Vortex Shedding
  Strouhal Number Prediction
  Variable vs Fixed Time Period Solutions
- Pitching Airfoil
  Steady/Unsteady Solutions vs Experimental Data
  NLFD vs Dual Time Stepping Codes (UFLO82)
- Conclusions

Navier-Stokes Equations

- The non-dimensional form of the governing equations.

$$\frac{\partial}{\partial t}\int_{\Omega} W \, dV + \oint_{\partial\Omega} \vec{F}_c \cdot \vec{N} ds = \sqrt{\gamma}\frac{M_\infty}{Re_\infty}\oint_{\partial\Omega} \vec{F}_v \cdot \vec{N} ds$$

$$\begin{bmatrix} \rho \\ \rho u \\ \rho v \\ \rho E \end{bmatrix} \qquad \begin{bmatrix} \rho & (u_i - b_i) & \\ \rho u_1 & (u_i - b_i) & +p\delta_{i1} \\ \rho u_2 & (u_i - b_i) & +p\delta_{i2} \\ \rho E & (u_i - b_i) & +u_i p \end{bmatrix} \qquad \begin{bmatrix} 0 \\ \sigma_{i1} \\ \sigma_{i2} \\ u_j \sigma_{ij} + q_i \end{bmatrix}$$

- $\vec{b}$ represents the velocity of the control volume faces.

Discretization

- The finite volume approximation to the governing equations:

$$V \quad \frac{\partial W}{\partial t} + \underbrace{\sum_{cv} \vec{F}_c \cdot \vec{S}} - \underbrace{\sum_{cv} F_{ad} - \frac{\sqrt{\gamma} M_\infty}{Re_\infty} \sum_{cv} \vec{F}_v \cdot \vec{S}} = 0$$

$$V \quad \frac{\partial W}{\partial t} + \underbrace{F_c + F_d} = 0$$

$$V \quad \frac{\partial W}{\partial t} + R(W) = 0$$

- Assume that the control volume may translate rigidly through space. Cell volume is not a function of time.

Frequency Domain Equations

- Represent W and $R(W)$ by a Fourier series in time.

$$W = \sum_{k=-\frac{N}{2}}^{\frac{N}{2}-1} \hat{W}_k e^{ikt} \qquad R(W) = \sum_{k=-\frac{N}{2}}^{\frac{N}{2}-1} \hat{R}_k e^{ikt}$$

- Resulting in a stationary system of equations in the frequency domain (NLFD).

$$ikV\hat{W}_k + \hat{R}_k = 0$$

- A second transformation back into the temporal domain results in Hall's harmonic balance approach.

$$S_n + R(W_n) = 0 \qquad S_n = iV \sum_{k=-\frac{N}{2}}^{\frac{N}{2}-1} k\hat{W}_k e^{ikt_n}$$

NLFD vs Harmonic Balance

- NLFD and harmonic balance methods converge to identical answers.
- Both approaches require the same amount of work per solver iteration.
  N residual evaluations based on N instances of the solution.
  2 FFTS are needed for either approach.
- Unlike harmonic balance techniques, the NLFD method advances the unsteady residual in the frequency domain affording a separate pseudo time step for each wavenumber that includes the effect of the temporal derivative on the stability of the system.
- The NLFD method simplifies the implementation of convergence acceleration techniques like implicit residual averaging and multigrid (using spectral viscosity).

Solver Implementation

- Since we are dealing with solving a steady system of equations, we apply established methods to accelerate the convergence.
    - Multi-stage RK scheme with local time stepping
    - Implicit residual averaging
        - CFL limiters
    - Multigrid V or W Cycle
        - Coarse grid spectral viscosity
- We are dealing with real functions where the Fourier coefficients for the positive wavenumbers are equal to the complex conjugates of the Fourier coefficients for the negative wavenumbers. This eliminates the computation required to integrate the negative wave numbers forward in pseudo-time.

Unsteady Residual

- Restating the governing equation in the frequency domain.

$$ikV\hat{W}_k + \hat{R}_k = 0 \qquad\qquad k = 0 \ldots N_{modes}$$

- Add in a pseudo time derivative:

$$V\frac{\partial \hat{W}_k}{\partial \tau} + \underbrace{ikV\hat{W}_k + \hat{R}_k}_{\hat{I}_k} = 0$$

- This gradient will iteratively adjust the solution in the frequency domain to minimize the magnitude of the unsteady residual $\hat{I}_k$.

Pseudo Spectral Approach

- The process of forming the unsteady residual is complicated by the nonlinearities included within the spatial operators.

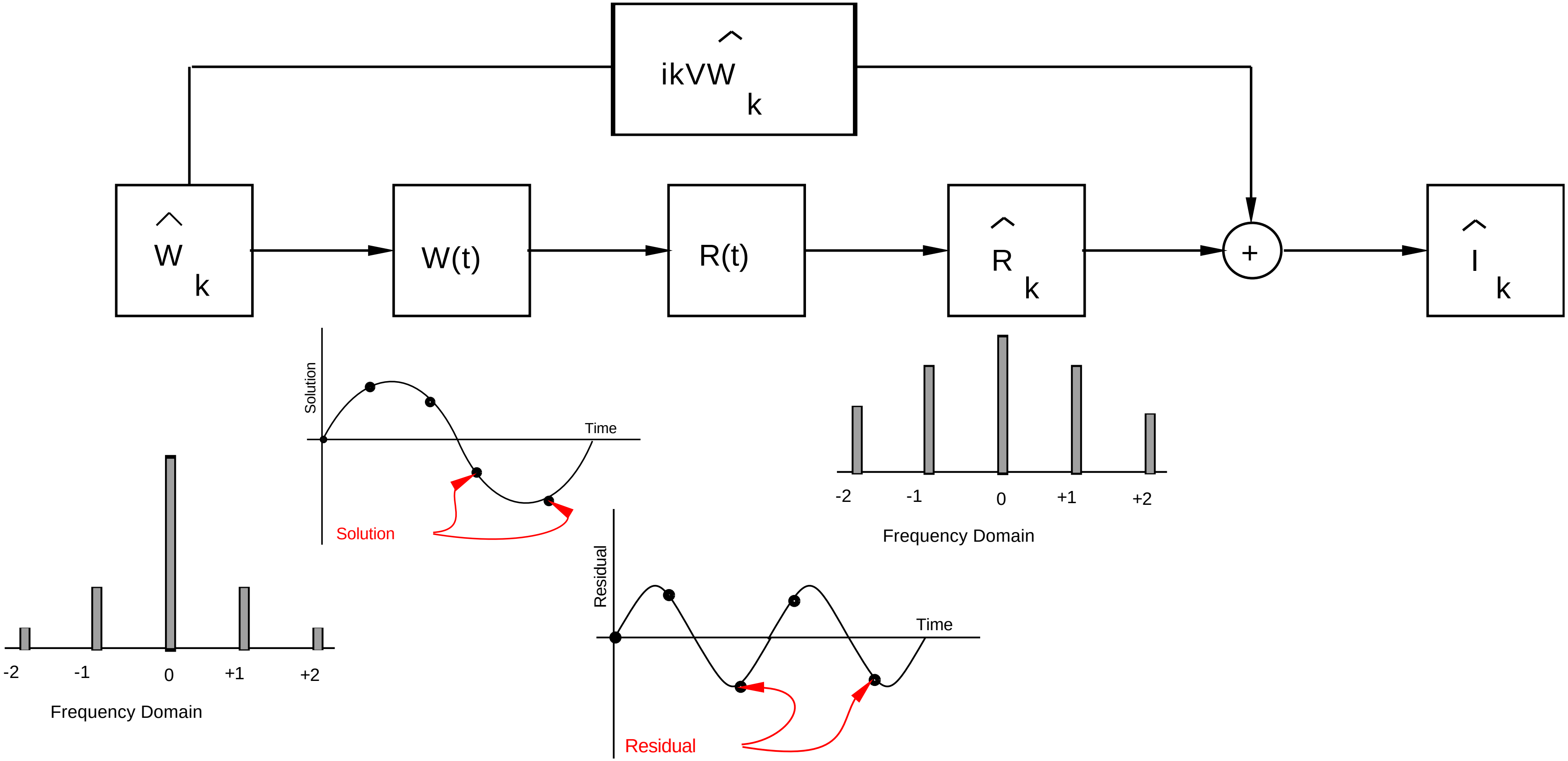

Multi-Stage RK Scheme

- Implementation of a multi-stage RK scheme for a stationary system of equations (Jameson 83).

$$W^m = W^0 + \Delta\tau\alpha^m \left(\frac{\partial W^m}{\partial \tau}\right)$$

$$\frac{\partial W^m}{\partial \tau} = F_c(W^m) + \beta^m F_d(W^m) + (1-\beta^m)F_d^{m-1}$$

- As applied in the frequency domain.

$$\hat{W}_k^m = \hat{W}_k^0 + \Delta\tau_k\alpha^m \left(\frac{\partial \hat{W}_k^m}{\partial \tau}\right)$$

$$\frac{\partial \hat{W}_k^m}{\partial \tau} = \frac{1}{N}\sum_{n=0}^{N-1}\left(F_c(W_n^m) + \beta^m F_d(W_n^m) + (1-\beta^m)F_{d_n}^{m-1}\right)e^{-ikt_n}$$

Implicit BDF

- Implicit treatment of an A-stable discretization (Melson 93).

$$-V\frac{\partial W_{n+1}^{m}}{\partial \tau} = V\frac{3W_{n+1}^{m} - 4W_n + W_{n-1}}{2\Delta t} + R(W_{n+1}^{m})$$

$$W_{n+1}^{m+1} = W_{n+1}^{0} - \frac{\alpha^m \Delta\tau}{V}\left(V\frac{3W_{n+1}^{m+1} - 4W_n + W_{n-1}}{2\Delta t} + R(W_{n+1}^{m})\right)$$

Explicit

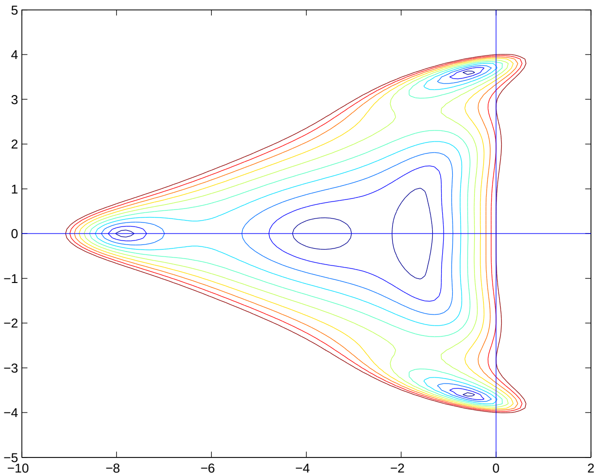

Implicit

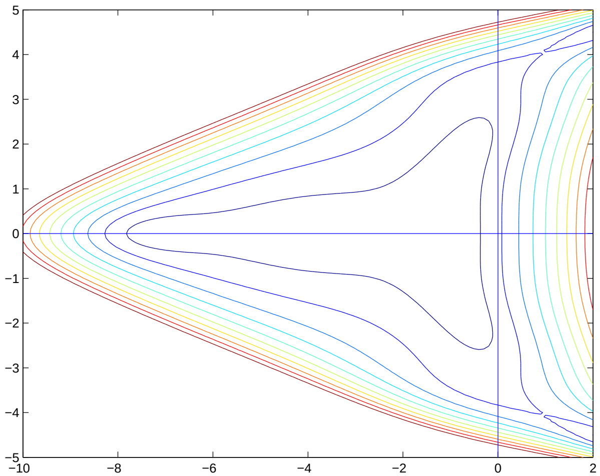

Implicit NLFD

- Implicit treatment of an NLFD method.

$$-V\frac{\partial \hat{W}_k^m}{\partial \tau} = ikV\hat{W}_k^m + \hat{R}_k(W^m)$$

$$\hat{W}_k^{m+1} = \hat{W}_k^0 - \frac{\alpha^m \Delta\tau_k}{V}\left(ikV\hat{W}_k^{m+1} + \hat{R}_k(W^m)\right)$$

Explicit | Implicit

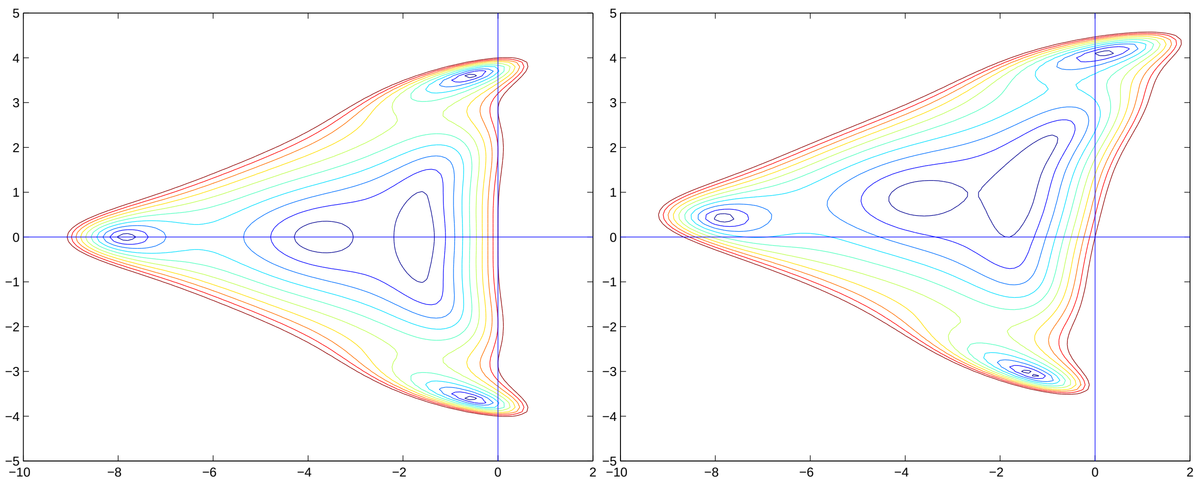

Residual Averaging - Frequency

- Continuous form of residual averaging for the advection equation.

$$\left(1 - e\frac{\partial^2}{\partial \eta_i^2}\right)\Delta\tau \bar{I} = -\Delta\tau\left(\frac{\partial u}{\partial t} + c\frac{\partial u}{\partial x_i}\right)$$

- Discrete operators for the above equation.

$$\begin{aligned} - e_k\Delta\tau_k\hat{\bar{I}}_{k_{i+1}} + (1+2e_k)\Delta\tau_k\hat{\bar{I}}_k - e_k\Delta\tau_k\hat{\bar{I}}_{k_{i-1}} &= \\ -\Delta\tau_k\left(ik\hat{u}_k + c\frac{\hat{u}_{k_{i+1}} - \hat{u}_{k_{i-1}}}{2\Delta x_i}\right)& \end{aligned}$$

Semi-Implicit Form

- Perform a von Neumann analysis to obtain the eigenvalue as a function of the discrete solution’s frequency.

$$\underbrace{\Delta\tau_k \hat{\hat{I}}_k} = \underbrace{\frac{k\Delta\tau_k + \Lambda_k sin(\rho)}{1 + 2e_k\left(1 - cos(\rho)\right)}} i\hat{u}_k$$

$$\Delta\tau_k \frac{\partial \hat{u}_k}{\partial \tau} = \lambda \hat{u}_k$$

- The above equation has been recast into a semi-implicit form suitable as the basis of a stability analysis.

CFL Limiter

- Resulting in a simple equation for the averaging coefficient e.
  $e \to \infty$ as $\pi\gamma \to 1$.

$$e_k = \frac{1}{4}\left(\frac{\pi^2 - (\pi\gamma)^2 + 2\pi\gamma - 1}{1 - \pi\gamma}\right)$$

$$\Lambda_k = \frac{c\Delta\tau_k}{\Delta x} \qquad \pi = \frac{\Lambda_k}{\mid \lambda \mid} \qquad \pi\gamma = \frac{k\Delta\tau_k}{\mid \lambda \mid}$$

- If residual averaging and multigrid are used simultaneously then the time step is calculated as:

$$\Delta\tau_k = min\left(\frac{\Lambda_0 V}{c + kV}, \frac{\mid \lambda \mid}{k}\right)$$

Spectral Viscosity

- The residual on the coarse mesh is defined as:

$$-\frac{\partial \hat{W}_k^m}{\partial \tau} = A_{2h}^h \hat{I}_k(W_h) - \hat{I}_k(A_{2h}^h W^0) + \hat{I}_k(A_{2h}^h W^m)$$

- If the restricted residual is zero then the coarse grid correction will always be zero.
  The ultimate driver in the multigrid cycle is the fine grid residual.
- Many steady-state multigrid codes take advantage of this by implementing third-order spatial dissipation operators on the fine grid and first order operators on the coarse grid.
- The additional dissipation improves the high frequency damping of the multigrid scheme resulting in an improved coarse grid correction.

Spectral Viscosity

- Add temporal damping on the coarse grid equations.

$$V \frac{\partial \hat{W}_k}{\partial \tau} + ikV\hat{W}_k + \hat{R}_k = \varepsilon V (ik)^{2s} \hat{W}_k$$

- This will mitigate the dependence of the convergence rate of the residual on the unsteady terms without affecting the solution.

Without SV

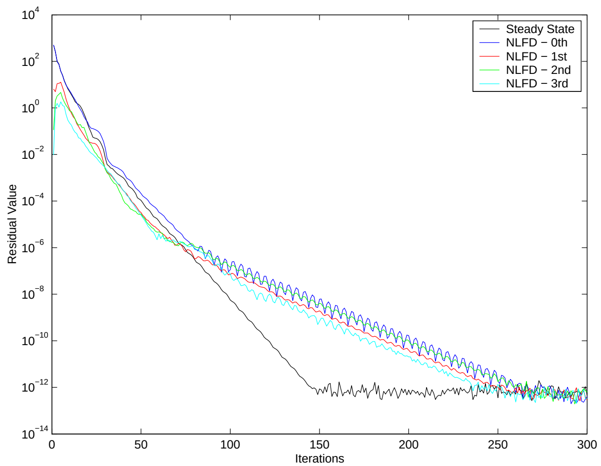

With SV

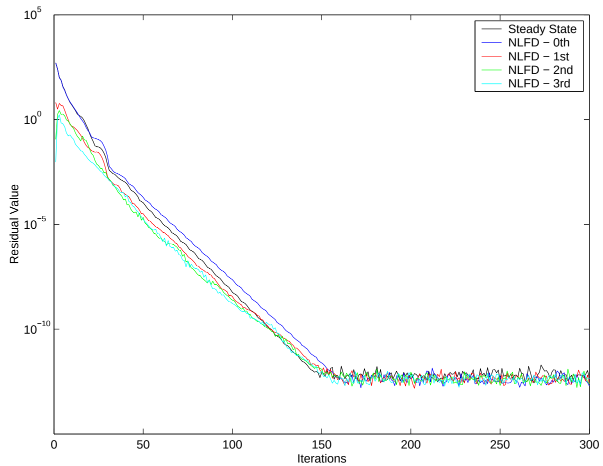

Unforced Problems

- In the development of the nonlinear frequency domain method, we assume the time period of the fundamental harmonic.
- A class of problems exists where the exact frequency of the phenomena described by discretized equations can not be known in advance. This research has developed the Gradient Based Variable Time Period (GBVTP) method to solve for the time period of the fundamental harmonic as part of the iterative solution process.
- The process of finding a solution to the unsteady flow equations is analogous to an optimization problem where the magnitude of the unsteady residual is minimized.
- Taking a derivative of the square of the magnitude of the unsteady residual with respect to the time period will form a gradient that will allow us to search for the time period that minimizes the unsteady residual.

GBVTP

- The normalized wavenumber k:

$$k = \frac{2\pi n}{T}$$

- The unsteady residual can then be written as a function of the time period T.

$$\hat{I}_n = \frac{i2\pi nV}{T}\hat{W}_n + \hat{R}_n$$

- The magnitude of the unsteady residual can be expressed as

$$\frac{1}{2}\frac{\partial\left|\hat{I}_n\right|^2}{\partial T} = \hat{I}_{nr}\frac{\partial\hat{I}_{nr}}{\partial T} + \hat{I}_{ni}\frac{\partial\hat{I}_{ni}}{\partial T}$$

GBVTP

$$\frac{\partial \hat{I}_{nr}}{\partial T} = \frac{2\pi n V \hat{W}_{ni}}{T^2} \qquad \frac{\partial \hat{I}_{ni}}{\partial T} = -\frac{2\pi n V \hat{W}_{nr}}{T^2}$$

- The gradient can be simplified by employing cross product notation.

$$\frac{1}{2}\frac{\partial \left|\hat{I}_n\right|^2}{\partial T} = \frac{2\pi n V}{T^2}|\vec{I_n} \times \vec{W_n}|$$

- By selecting a stable ΔT the gradient information can be used to update the time period after each multigrid cycle in the solution process.

$$T^{n+1} = T^n - \Delta T \frac{\partial \left|\hat{I}_n\right|^2}{\partial T}$$

Cylinder - Motivation

- To show that the NLFD method using a limited number of time varying modes could accurately resolve complex flow field physics such as the von Kármán vortex street.
- To demonstrate the ability of the GBVTP method to automatically determine the shedding frequency of the discrete equations.
- To show the impact of the GBVTP method on the solution in comparison to fixed time period results.

Cylinder - Experiment

- Laminar vortex shedding occurs behind a circular cylinder over a range of Reynolds numbers between 40 and 194 (Williamson).

Side View

Source:Taneda

Top View

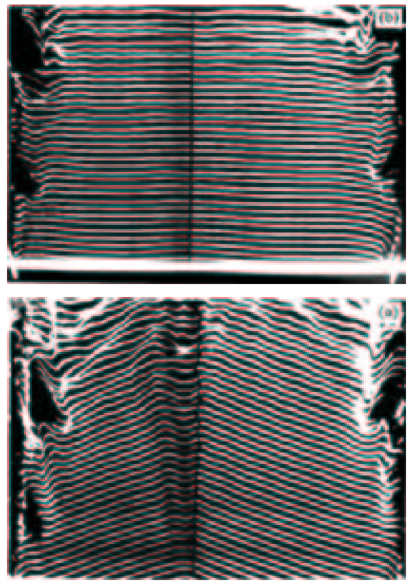

Source:Williamson

- It is important to note the cylinder end boundary conditions when selecting experimental studies for comparison.

Cylinder - Details

Nearfield - 257x129

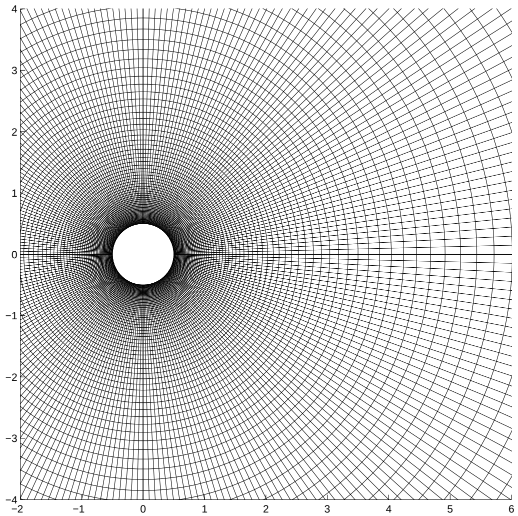

Entropy contours

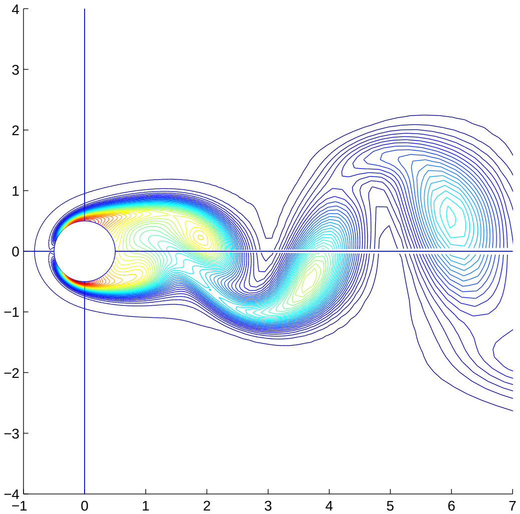

- Three dimensional parametric survey:

Variable	Values
Temporal Resolution	1,3,5,7
Grid Resolution	129x65,193x81,257x129,385x161
Reynolds Number	60,70,80,90,100,110,120,130,140,150

Strouhal Predictions

193x81 grid

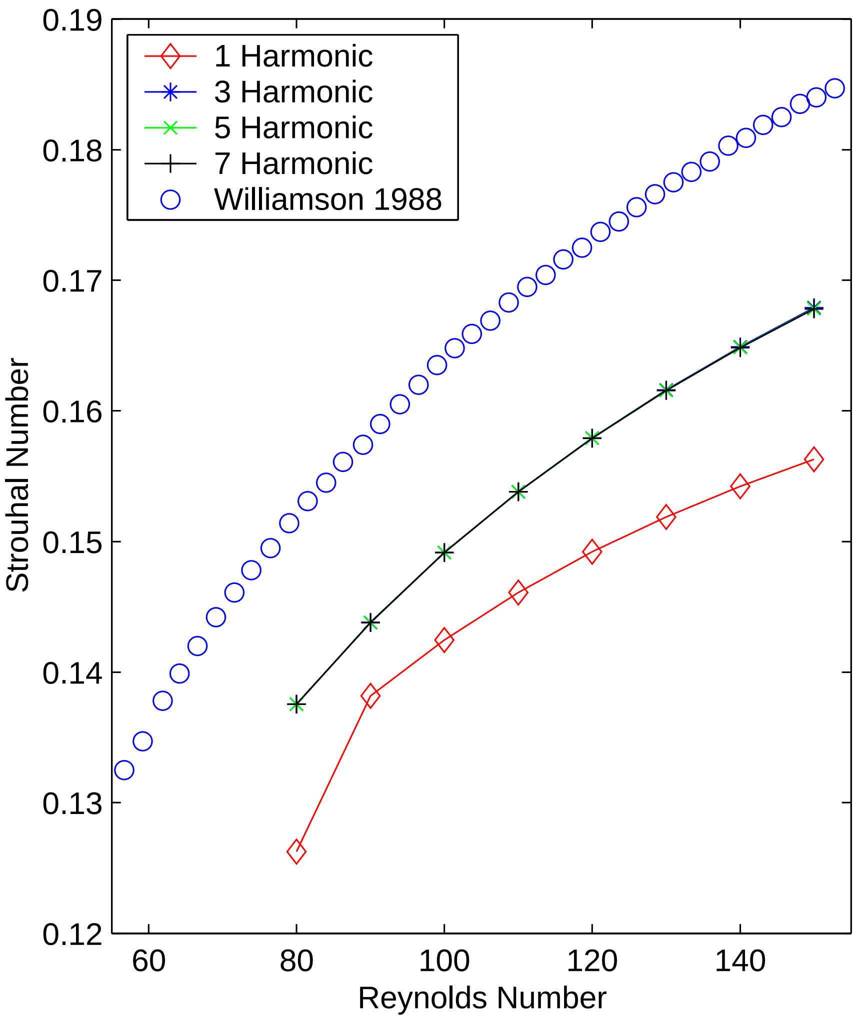

385x161 grid

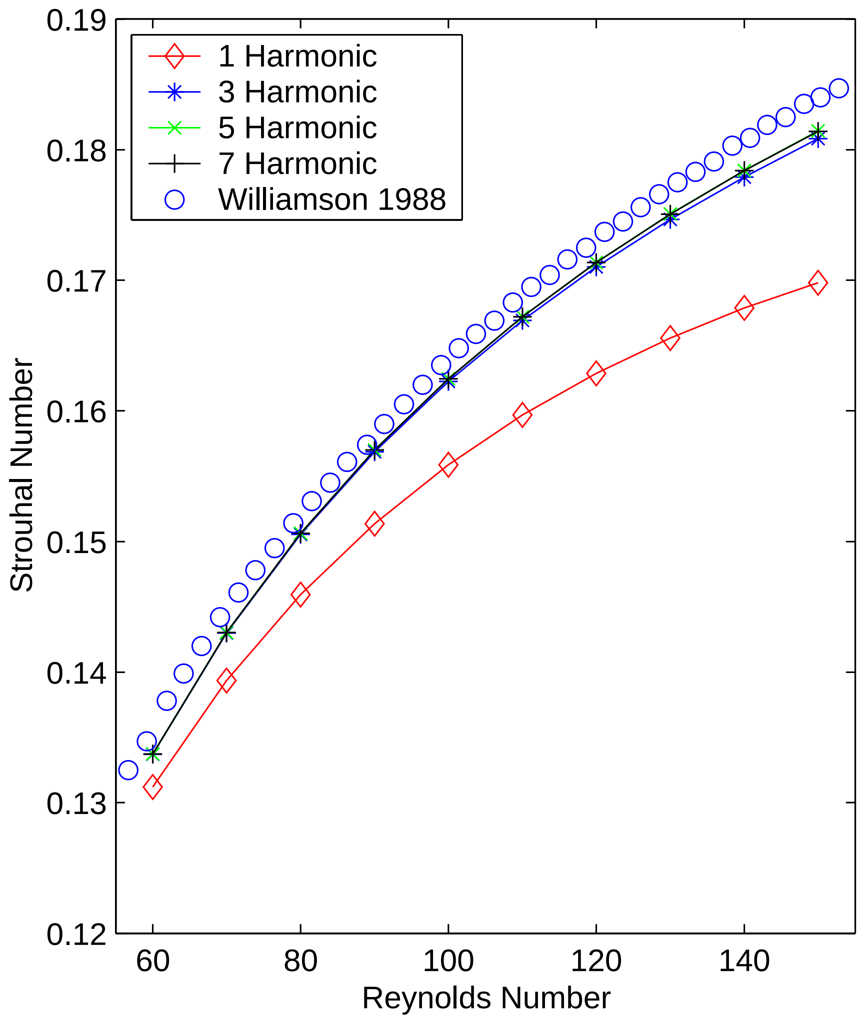

Residual vs Strouhal

- The GBVTP method will find the exact Strouhal number for the discrete equations. Performing a fixed Strouhal number calculation without using the exact Strouhal number will result in a non-zero unsteady residual.

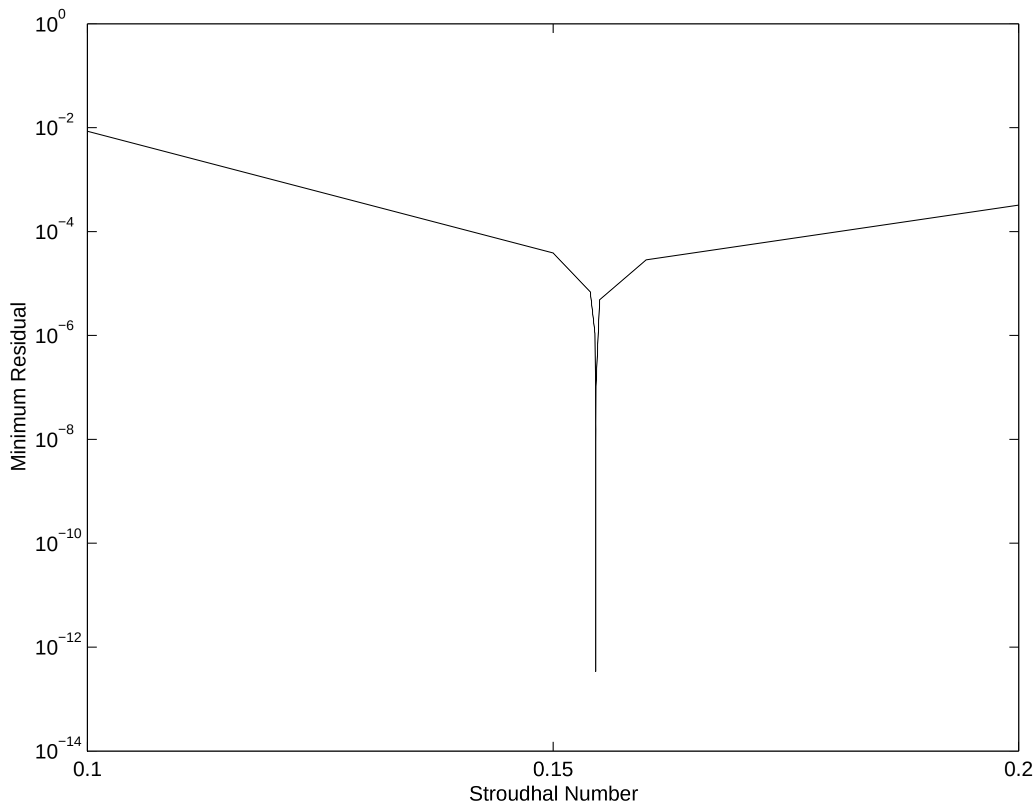

Base Suction Coefficient - C_{p_b}

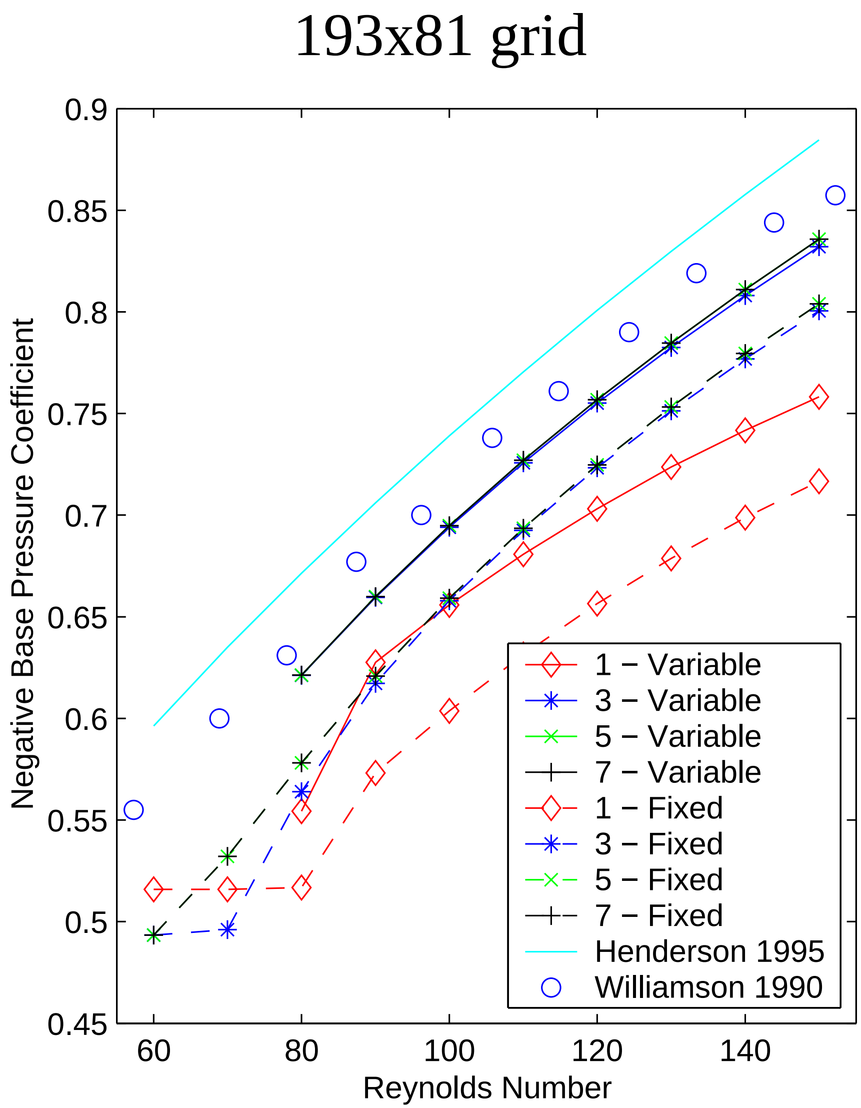

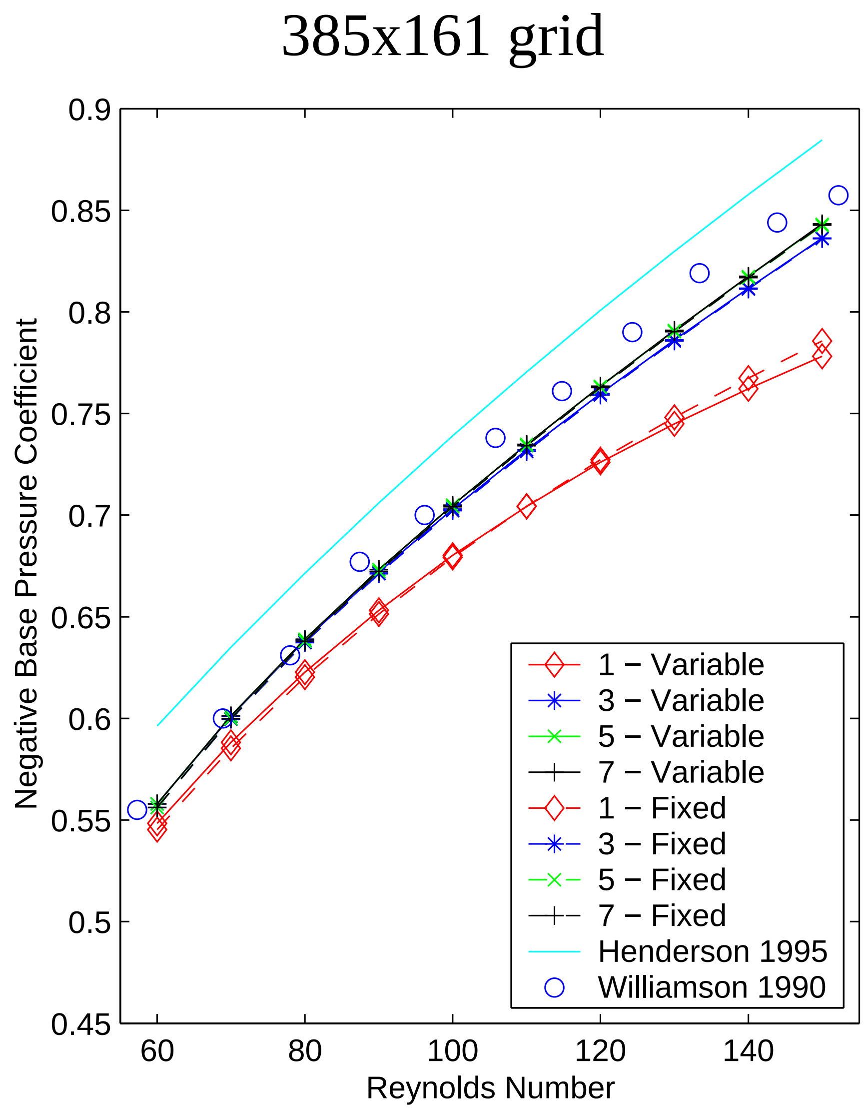

Airfoil - Motivation

- To demonstrate the ability of the NLFD method to time accurately resolve flows of engineering importance like a transonic pitching airfoil in inviscid and turbulent viscous environments.
  Euler simulations
  Turbulent Navier-Stokes - Baldwin/Lomax model
- To compare the efficiency of the NLFD solver to time accurate codes like UFLO82 which implements a dual time stepping technique.

Airfoil - Experiment

Description	Variable	Green	Davis	Landon
Airfoil		0012	64A010	0012
Case Number		Slotted 119 134 Adaptive 201	CT Case 6 DI 55	CT Case 1
Mean Angle of Attack	α	$-2.0^\circ - 6.0^\circ$	0.0° $\pm 1.01^\circ$	2.89° $\pm 2.41^\circ$
Reynolds Number	Re_∞	3.0×10^6 9.0×10^6	12.56×10^6	4.8×10^6
Mach Number	M_∞	0.7	0.796	0.6
Reduced Frequency	k_c	0	0.202	0.0808

NACA 0012 Steady C_l

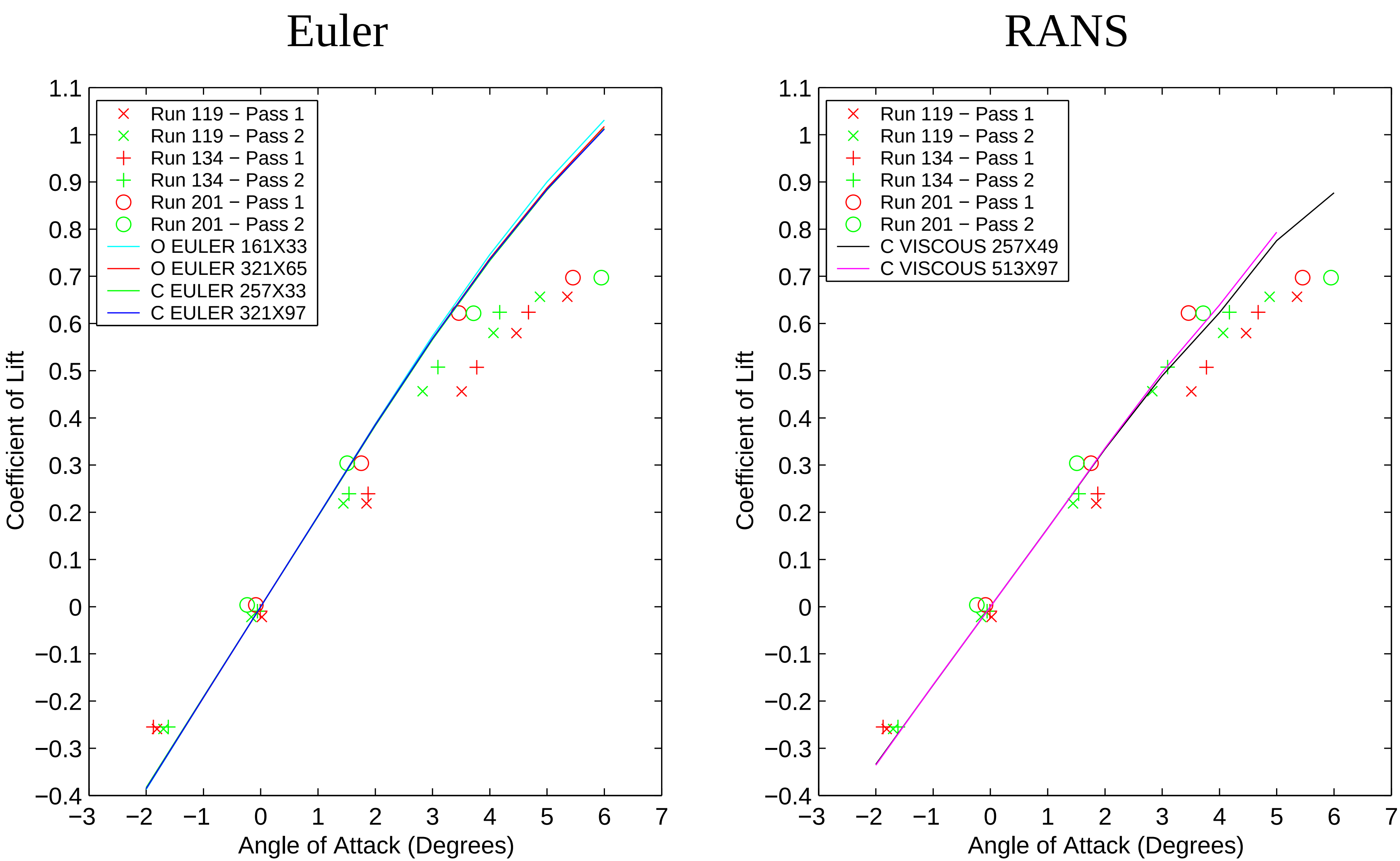

NACA 0012 Steady C_m

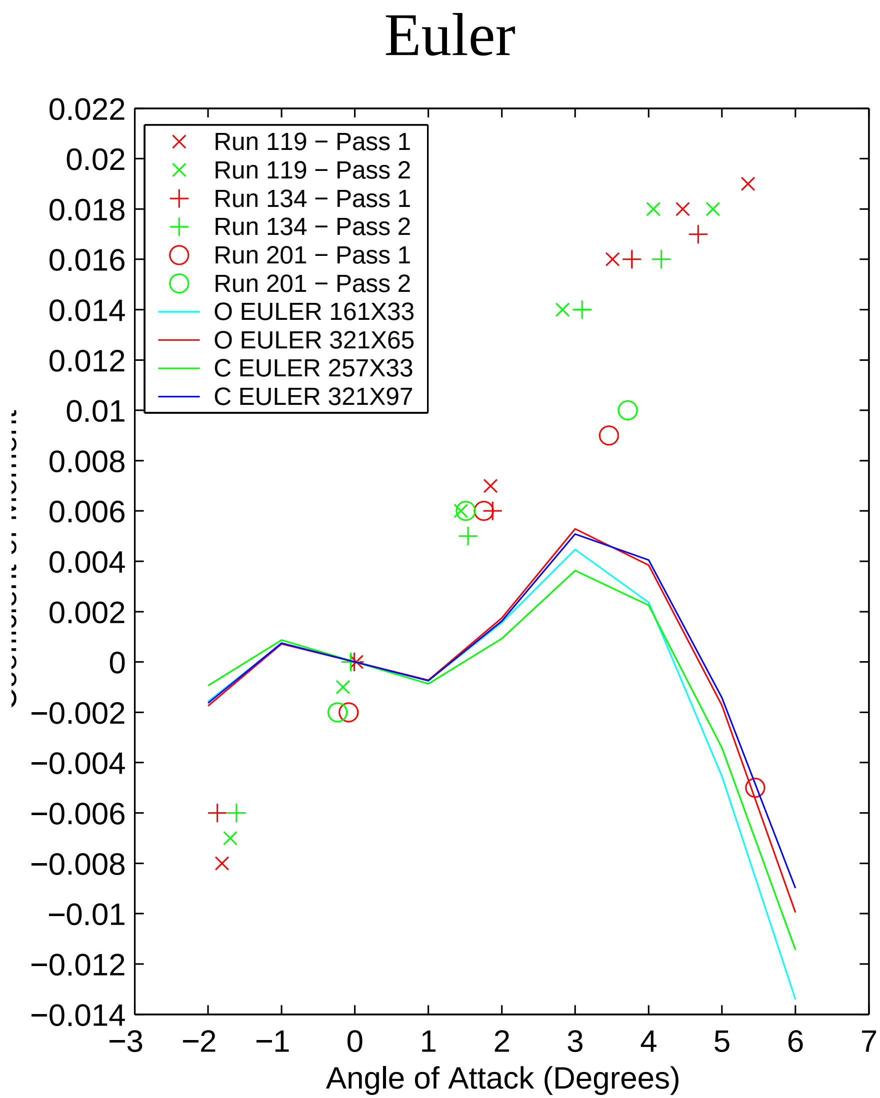

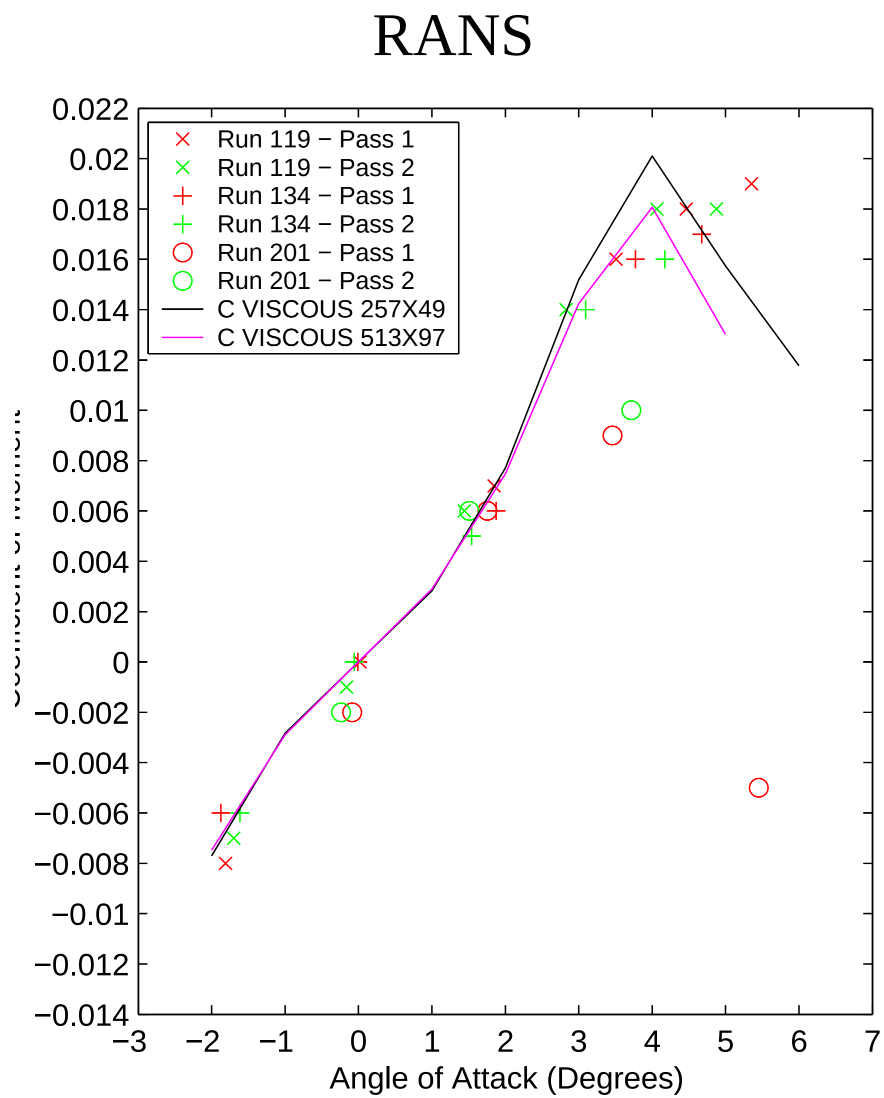

NACA $64A010$ Unsteady C_l

Euler

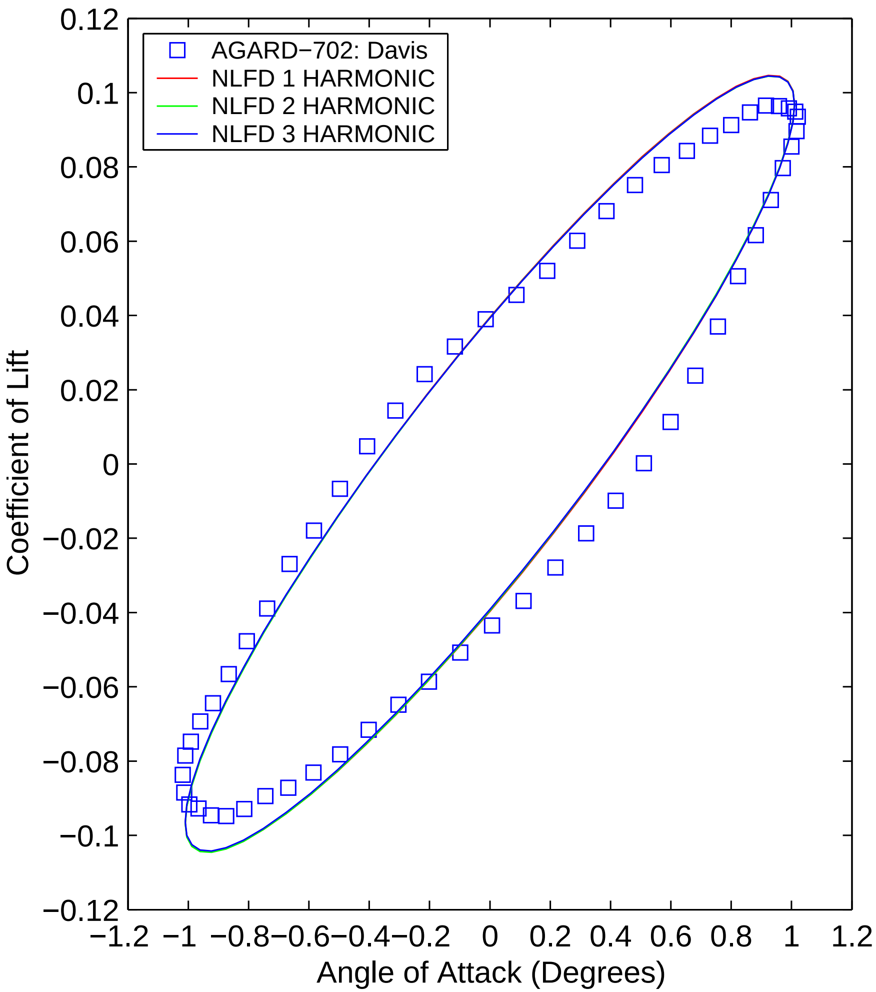

RANS

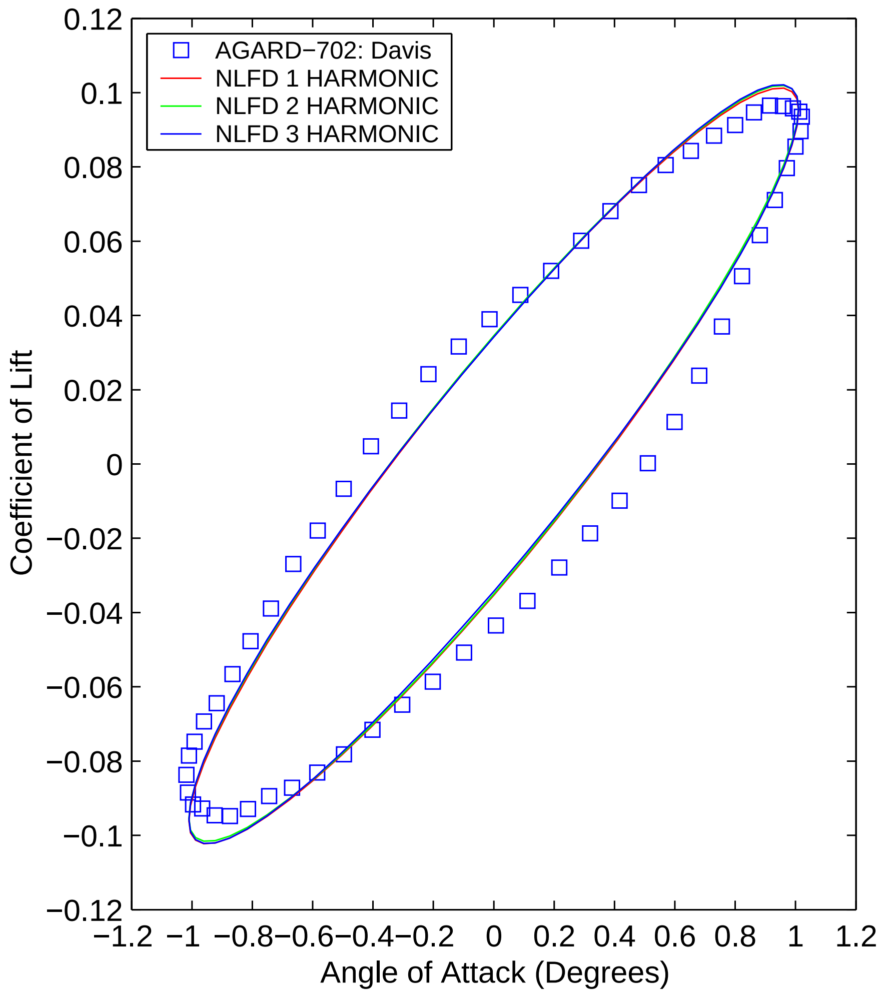

NACA $64A010$ Unsteady C_m

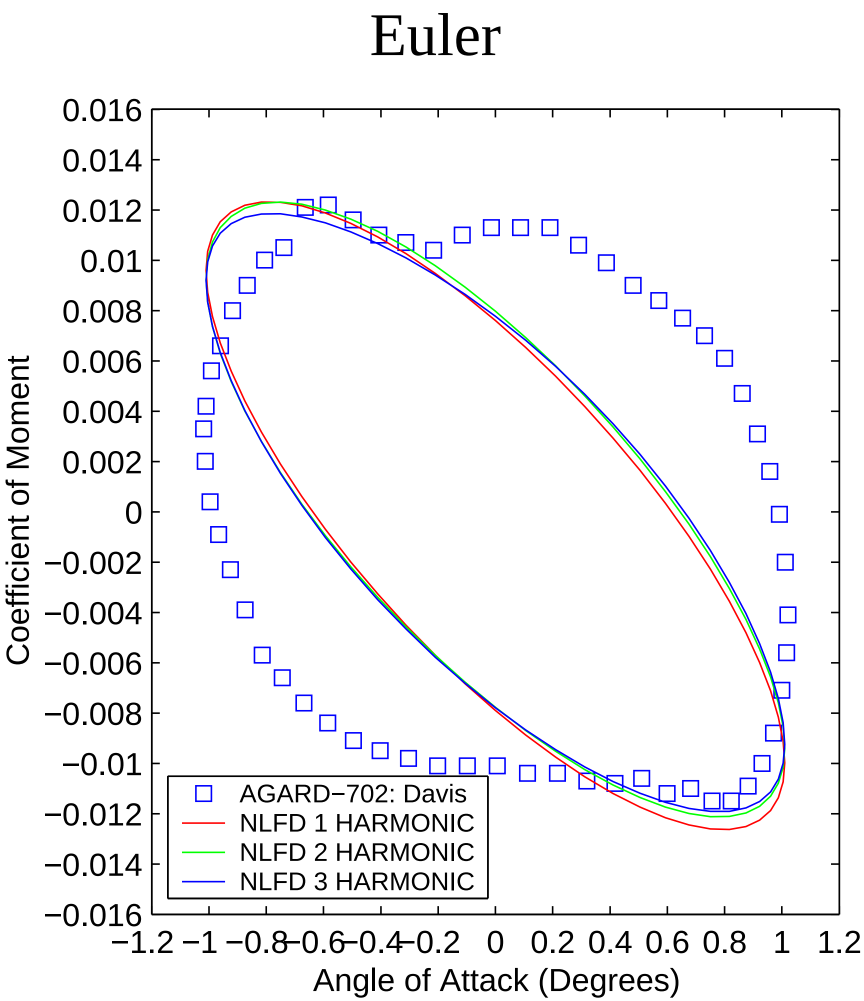

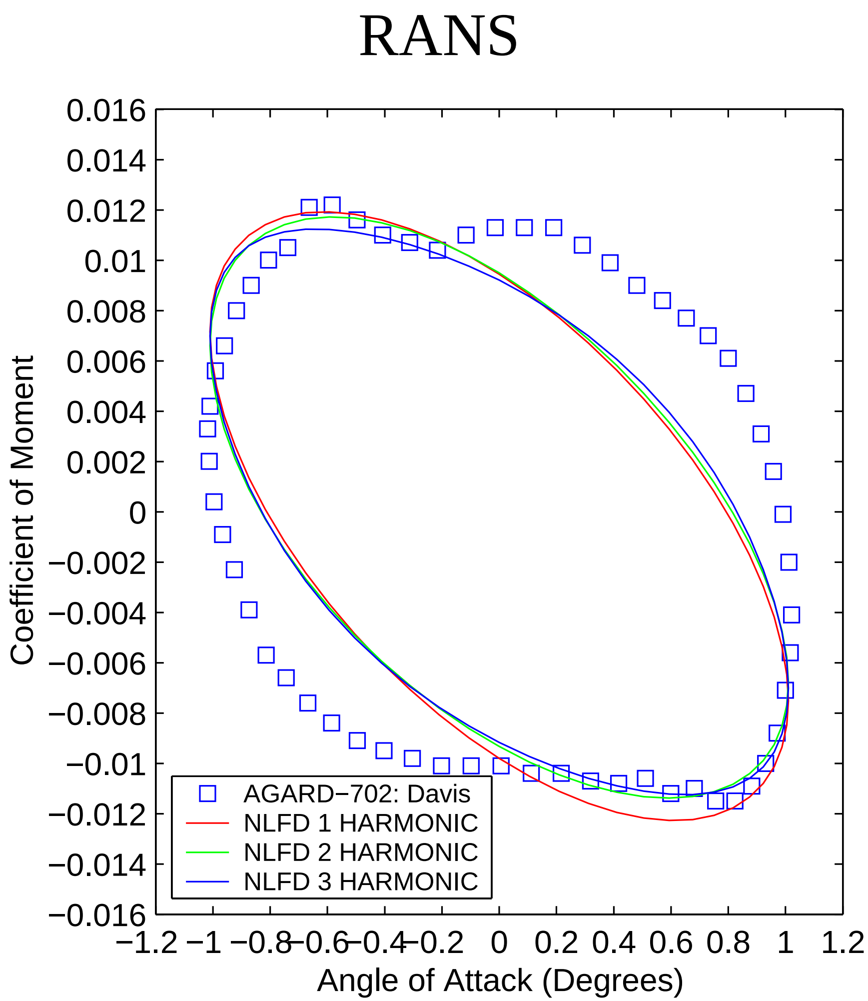

UFLO82 vs NLFD

- A study was carried out to compare the efficiency of UFLO82 and the NLFD solver.
- Different time marching methods are commonly compared on the basis of the amount of error they produce. The comparison is constrained by advancing the solution forward an equivalent amount of time using an equal number of residual evaluations.

$$\frac{du}{dt} = \lambda u$$

$$u_{n+1} = u_{n-1} + 2\Delta t \frac{du_n}{dt} \qquad u_{n+1} = u_n + \frac{\Delta t}{2}\left(3\frac{du_n}{dt} - \frac{du_{n-1}}{dt}\right)$$

- This study compares the amount of work required by the different methods to obtain an equivalent level of error.

Residual Equivalence

- The difference in the solution (ρe) between an NLFD and UFLO82 steady calculation is $\mathcal{O}(10^{-13})$.

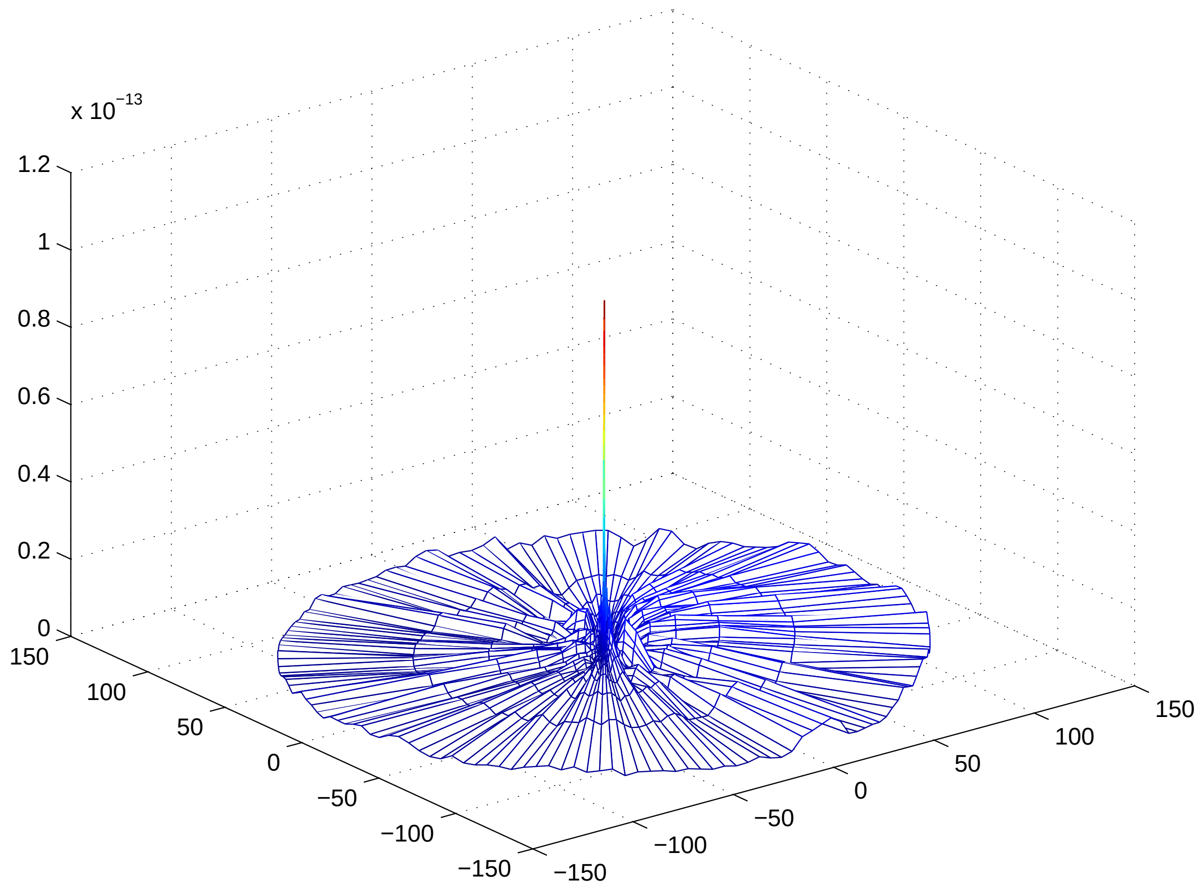

Error Definition

- The basis of comparison between the two codes will be the error in the magnitude of the Fourier coefficient of lift or moment.

$$
\begin{aligned}
E_{N_l} &= \left| |\hat{C}_{l_1}| - |\hat{C}_{l_{1_{512}}}| \right| \\
E_{N_m} &= \left| |\hat{C}_{m_1}| - |\hat{C}_{m_{1_{512}}}| \right|
\end{aligned}
$$

- The most accurate solution was produced from a 512 points per period (SPP) UFLO82 calculation. The residual was driven to machine zero at each physical step which advanced the solution 48 complete periods. Only the final period was used for the purposes of quantifying the error.

Test Case Details

- We will use a more challenging test case for the numerical comparison.
  Reduced frequency is lower. Angle of attack variation is higher

Parameter	Value
Airfoil	NACA 64A010
Mean Angle of Attack	0.0°
Angle of Attack Variation	$\pm 2.0^\circ$
Mach Number	0.8
Reduced Frequency	0.05

- All numerical computations will be carried out on a 161x33 O-mesh. The topology is constrained by the selection of the UFLO82 code.

UFLO82 Error Results

- Error between various temporal resolutions of the UFLO82 code and the control solution.

C_l

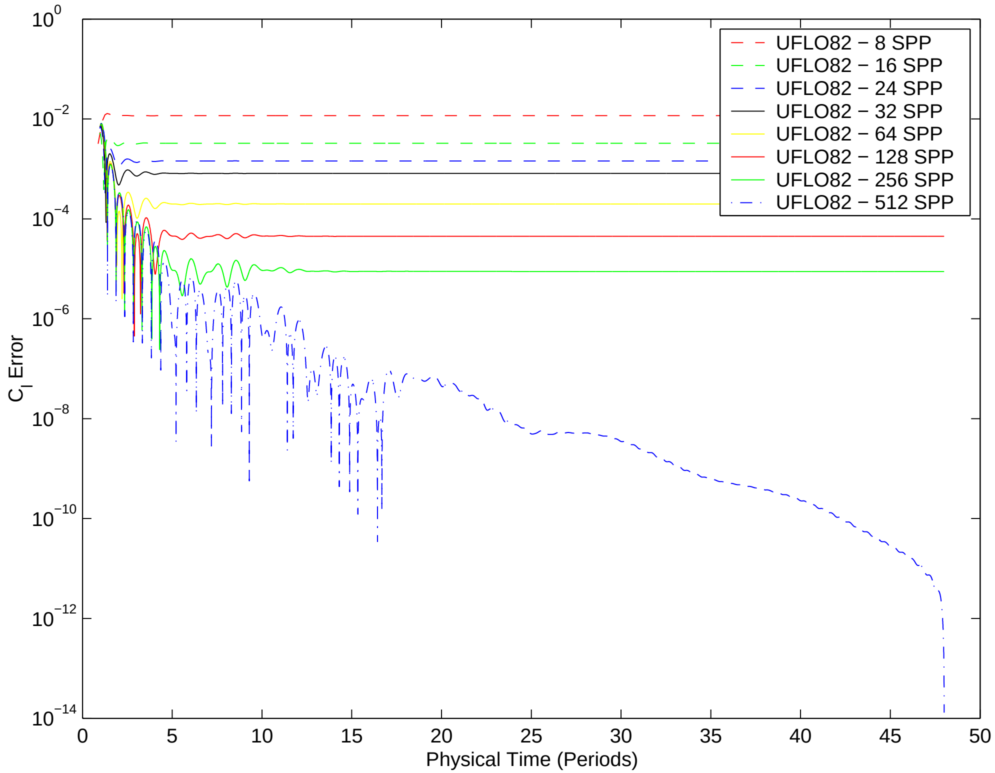

C_m

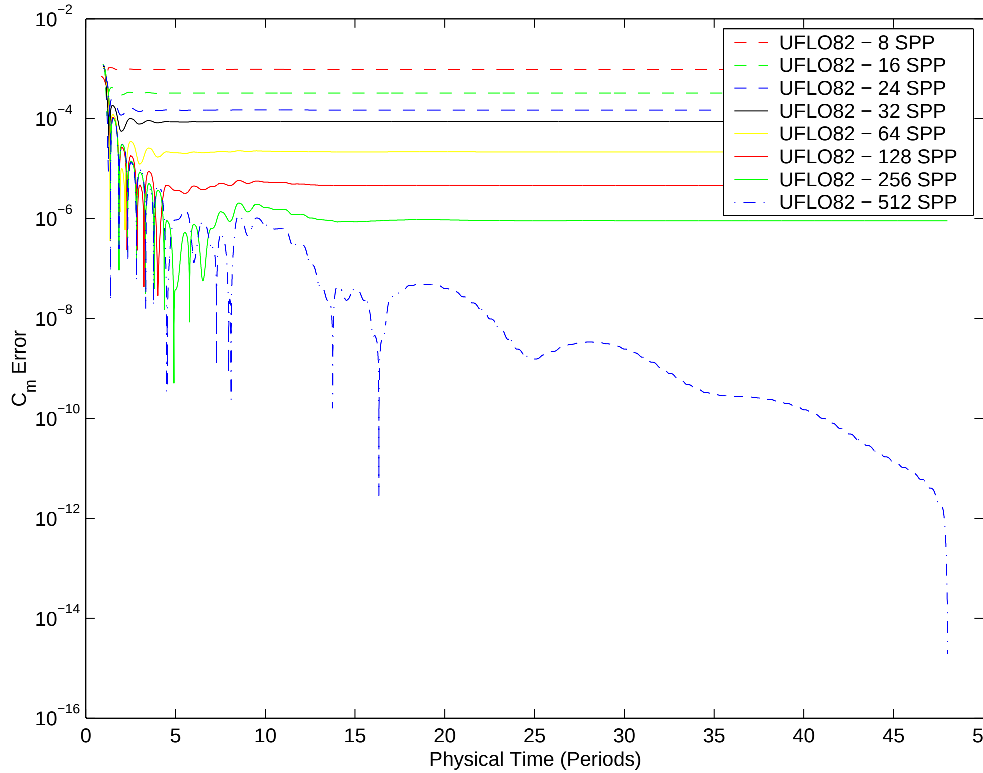

UFLO82 - Solutions per Period

- Asymptotic error in C_{l_1} and C_{m_1} computed at various temporal resolutions by the UFLO82 and NLFD codes.

C_l Error

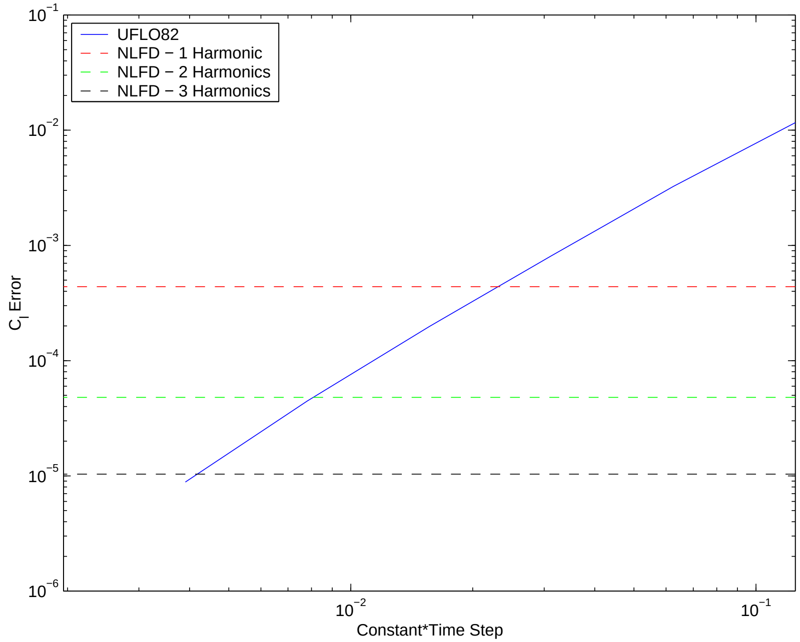

NLFD	1	2	3
UFLO82	45	125	244

$C_m Error$

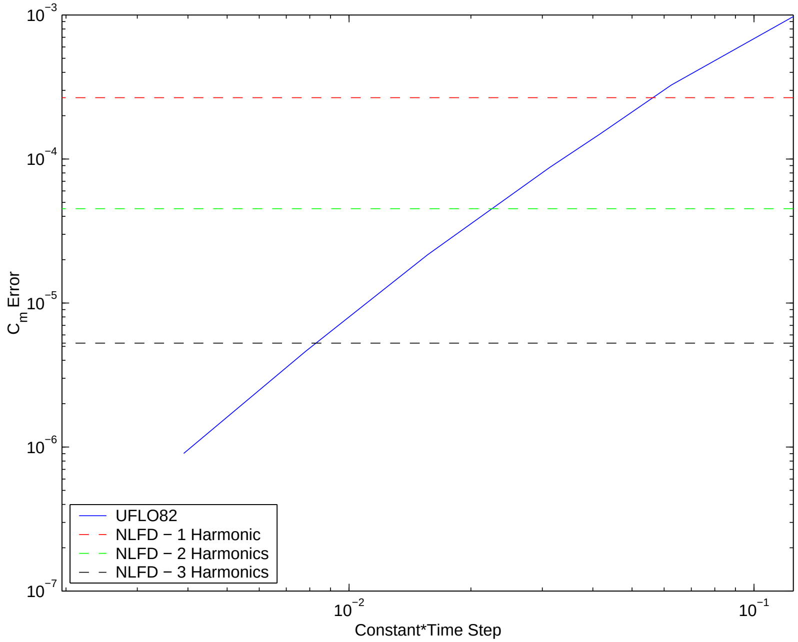

NLFD	1	2	3
UFLO82	18	45	123

Cost Estimates

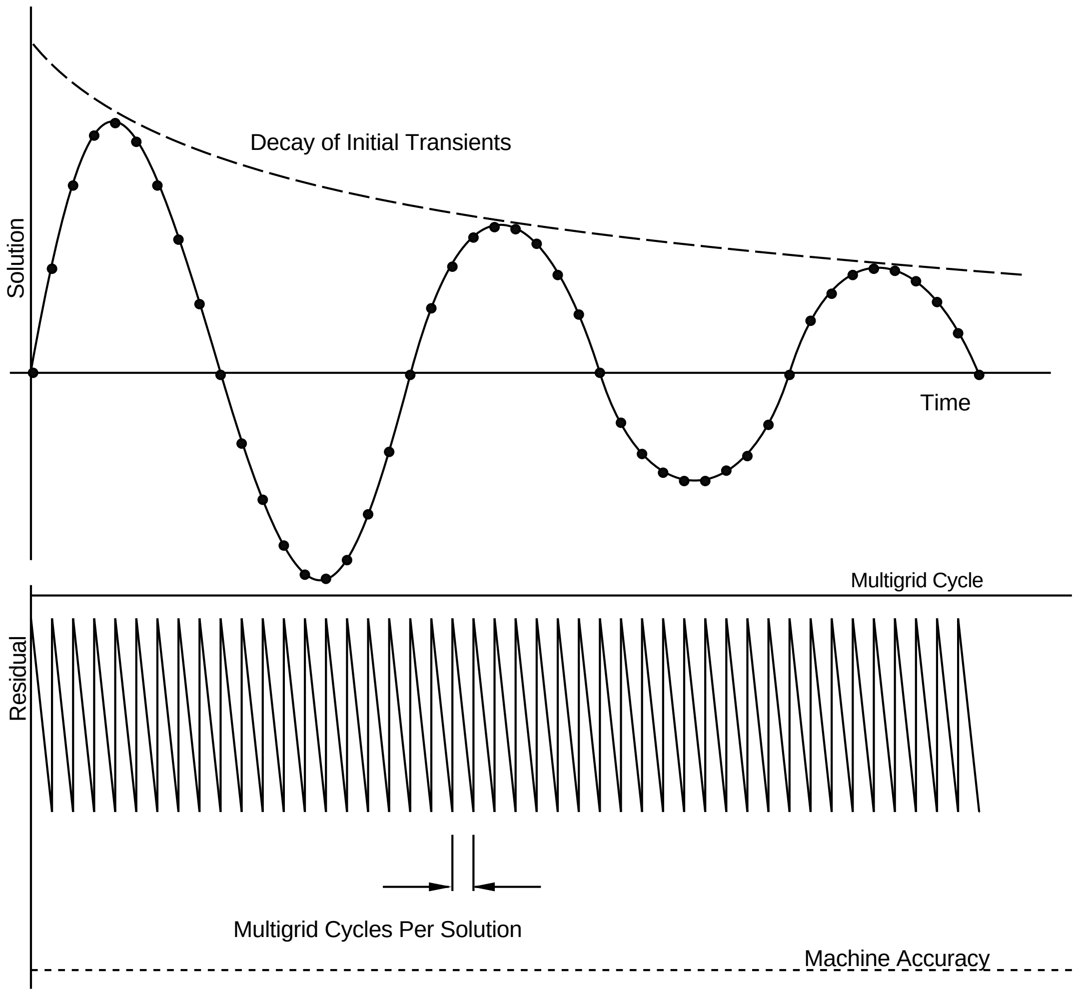

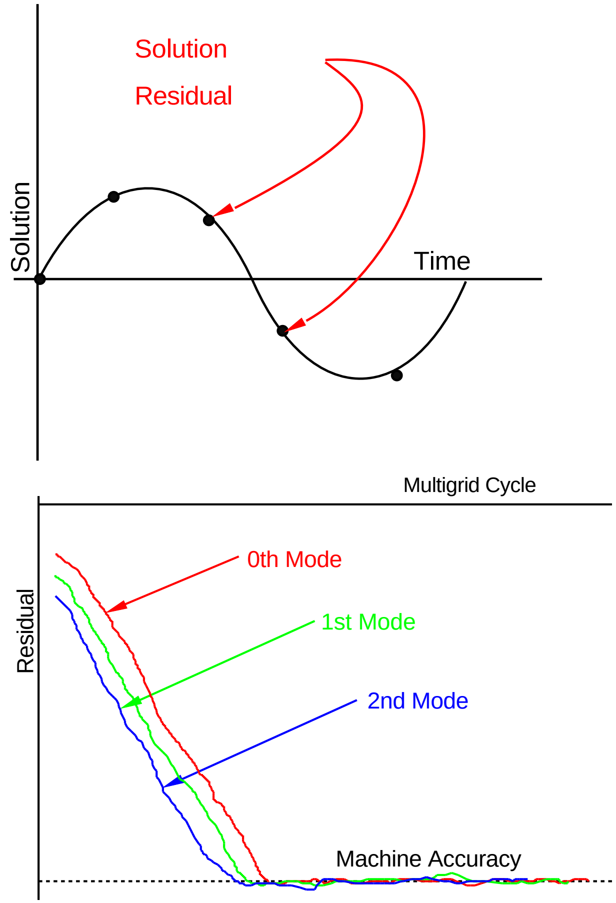

$$\frac{3W_{n+1} - 4W_n + W_{n-1}}{2\Delta t} + R(W_{n+1}) = 0 \qquad ikV\hat{W}_k + \hat{R}_k = 0$$

Cost Comparison - C_l

- Cost comparison using the error in C_l as the figure of merit.

NLFD Modes	Cost	UFLO82 SPP	Cost	Cost Ratio
1	$3.06 \times 44 = 135$	45	$4 \times 45 \times 6 = 1080$	8.0
2	$5.13 \times 60 = 308$	125	$5 \times 125 \times 6 = 3750$	12.2
3	$7.30 \times 72 = 526$	244	$7 \times 244 \times 6 = 10248$	19.5

$$\frac{Time\ \ n^{th}}{Time\ \ O^{th}} \times MultigridCycles$$

$$Periods \times \frac{Solutions}{Period} \times \frac{MultigridCycles}{Solution}$$

Cost Comparison - C_m

- Cost comparison using the error in C_m as the figure of merit.

NLFD Modes	Cost	UFLO82 SPP	Cost	Cost Ratio
1	$3.06 \times 37 = 113$	18	$3 \times 18 \times 6 = 324$	2.9
2	$5.13 \times 50 = 257$	45	$4 \times 45 \times 6 = 1080$	4.2
3	$7.30 \times 65 = 475$	123	$6 \times 123 \times 6 = 4428$	9.3

$$\frac{Time\ n^{th}}{Time\ O^{th}} \times MultigridCycles$$

$$Periods \times \frac{Solutions}{Period} \times \frac{MultigridCycles}{Solution}$$

Convergence Sensitivity

- This research has also studied the sensitivity of the residual convergence of the NLFD solver on physical aspects of the problem. Plotted is the maximum of the absolute value of the residual over all the wavenumbers .

Dynamic Angle of Attack

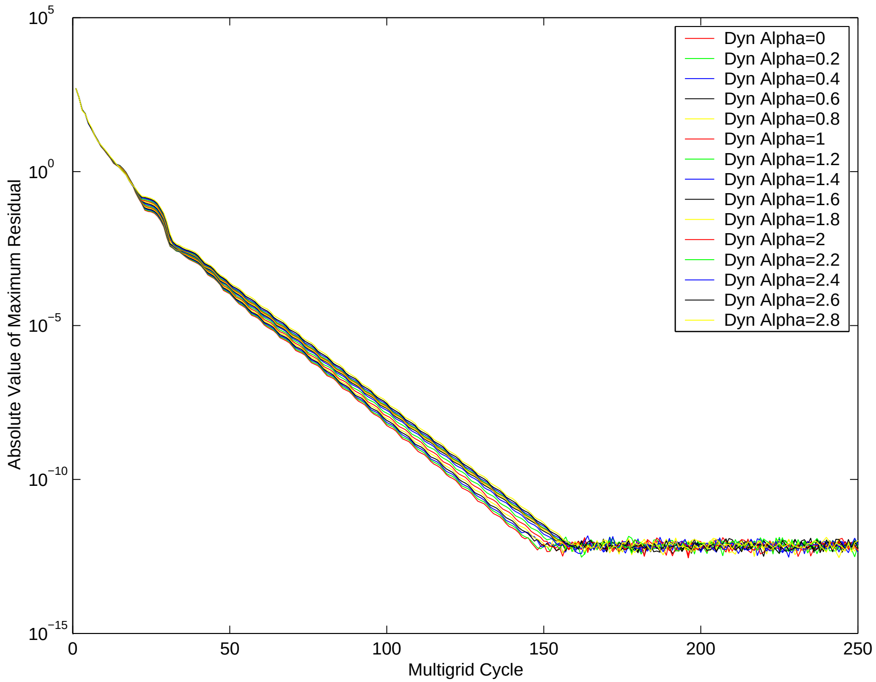

Reduced Frequency

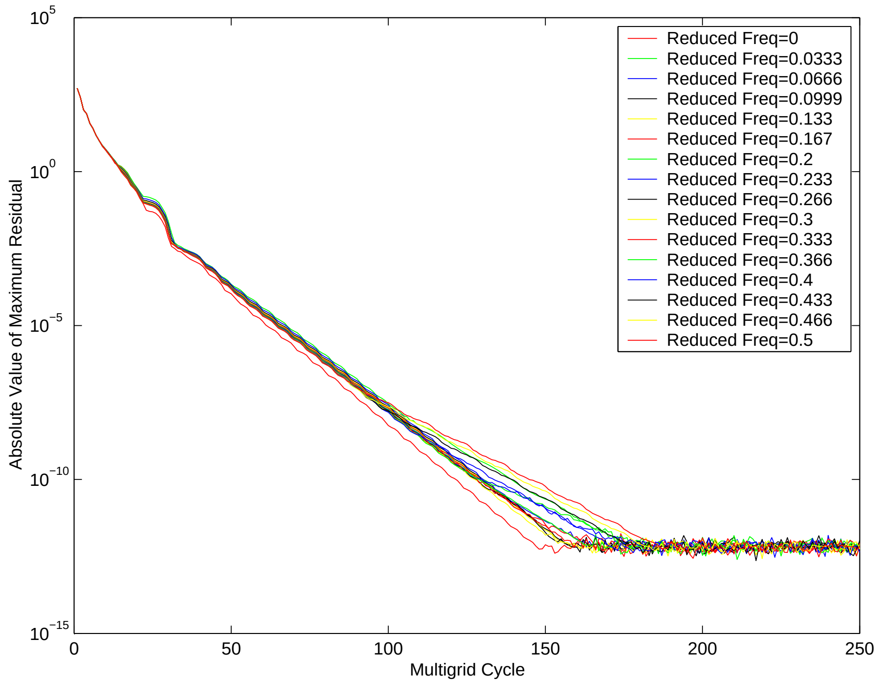

Implications for TFLO

- The Stanford ASCI project has already performed several unsteady viscous simulations of an experimental test rig using TFLO. Aachen turbine rig: Stator-rotor-stator : 6-7-6 model
- The NLFD estimates are based on 14 temporal modes and 600 multigrid cycles to achieve convergence.

Component	Multigrid Cycles	CPU Time (hrs)	Clock Time (hrs)
TFLO	123,630	371,000	1985[1]
NLFD	17,400	52,200	279[1]

[1] Clock time based on 187 processors.

Conclusion - Solver Details

- NLFD methods can be integrated into robust solvers exhibiting convergence performance close to that of more established steady state solvers.
- Multigrid should be modified with coarse grid spectral viscosity to mitigate the dependence of convergence rates on unsteady effects.
- The implicit treatment of the temporal derivative commonly found in dual time stepping codes is not recommended for NLFD solvers.
- Residual averaging should be modified with CFL limiters to ensure stability on coarse grids within the multigrid cycle.

Conclusion - Cylinder

- Three time varying modes are required to predict the Strouhal number and base suction coefficient to engineering accuracy for the entire range of laminar Reynolds numbers.
- The GBVTP method can be used to predict the time period of the fundamental harmonic.
- The GBVTP method improved the agreement between the numerical and experimental results for base suction coefficient in comparison to fixed time period methods.

Conclusion - Pitching Airfoil

- Using just one time varying mode, the NLFD predictions for coefficient of lift provide excellent agreement with experimental results.
- In the case of the coefficient of moment, NLFD predictions provide poor agreement with experimental studies.
- Given equivalent spatial discretizations and overall error, the NLFD method is significantly more efficient than dual time stepping codes like UFLO82.

Contributions

- The first to demonstrate a frequency domain solver for the laminar and turbulent Navier-Stokes equations.
- Independently developed an NLFD solver with convergence rates equivalent to state-of-the-art steady codes.
  Enabling technologies: Residual Averaging, Spectral Viscosity
  Multiple topologies : Parallel multiblock, O-mesh and C-mesh grids
  Multiple equations: Euler, laminar and turbulent Navier-Stokes
- The first to demonstrate the Gradient Based Variable Time Period (GBVTP) method.

Acknowledgments

- Antony Jameson and Juan Alonso
- ASCI program and William Reynolds
- Sanjiva Lele and George (Bud) Homsy
- Kenneth Hall
- Charles Williamson
- Sanford Davis
- Lawrence Green